# Study of Earth Dam Erosion due to Overtopping

F. MACCHIONE[1] and B. SIRANGELO[2]
[1]*Department of Soil Defence, University of Calabria,*
[2]*Institute of Civil Engineering, University of Salerno, Italy*

## Introduction

THE PROBLEM of dam failures has always been of great importance because of their disastrous effects. Therefore, it has always given rise to a particular interest among hydraulic engineers in order to estimate downstream valley areas exposed to the hazard of inundation.

Of great interest is the study of earthen embankment failures which are by far the most common type of dam in the world. A recent report has shown that the frequency of failure of such dams is about four times greater than that observed for concrete and masonry dams (Lebreton, 1985).

In Italy two recent events have drawn engineers' attention to the necessity of increasing the present knowledge about this matter:

- the failure of two settling reservoirs of a mining plant in Val di Stava, which caused heavy loss of human life; and
- the blocking of an upper reach of the Adda river in Valtellina, due to a landslide. In the latter event, overtopping of the embankment was kept under control by a Technical Commission of the Ministry of Civil Protection.

The present paper deals with an analysis of the interaction between reservoir routing and earth embankments in order to simulate the erosion process and evaluate and outflow hydrograph.

## Failure of Earthen Dams

Among the main causes of dam failures, besides floods exceeding the spillway capacity, may be included settlements, foundation failures, cracks, embankment slips and landslides falling into the reservoir. Many such conditions are due to earthquakes and they can also be joined to water reservoir waves (Sherard *et al.*, 1963; Johnson and Illes, 1976; Seed *et al.*, 1980).

Apart from their causes, failures can be followed by a water release either on the top of the dam (overtopping) or through the embankment (piping). In the latter case, seeping water makes a free path through the dam; this increases in size until the material above this hole collapses and the overtopping begins.

Observations of past dam failures have indicated that the breach shape is usually triangular and its width and depth grow during overtopping. In the case of earthfill dams, the breach can generally grow until it reaches the natural ground, which is less erodable, and then it develops laterally so its final shape will be trapezoidal. More complex and erratic is the breach development in earth dams with protective concrete surface layers and core walls (McDonald and Langridge-Monopolis, 1984).

It is important to point out that observed times for earth dam erosion show that breach growth is not a fast process. It is just this gradual character that distinguishes the failures of earthen embankments from those of concrete dams.

## Model Formulation

In the last 10 years several breach flood wave models have been developed with the purpose of simulating the outflow hydrograph and routing this hydrograph through the downstream valley. Concerning the breach simulation it is possible to distinguish the following methods (Wurbs, 1987):

- instantaneous complete removal of the dam;
- instantaneous partial breach of the dam;
- breach whose growth is fixed with time;
- breach whose growth is predicted using an erosion model.

The first two methods may be appropriate respectively for a concrete arch dam and for a concrete gravity dam, but they seem to be too conservative and unrealistic for earth embankments. The assumption that breach dimension grows with time, usually according to a linear law, appears more likely. However, the fourth method, adopted in the present paper, provides a more realistic representation of the erosion process.

Referring to the definition sketch in Figure 1, the flow of water over the dam can be described by the one-dimensional De Saint Venant equations:

$$\frac{\partial Q}{\partial x} + \frac{\partial A}{\partial t} + \frac{\partial A_d}{\partial t} = 0 \qquad (1)$$

$$\frac{\partial Q}{\partial t} + \frac{\partial}{\partial x}\left(\frac{Q^2}{A}\right) + gA\left(\frac{\partial Z}{\partial x} + S_f\right) = 0 \qquad (2)$$

where $Q$ is the discharge, $A$ is the cross-sectional area of water, $A_d$ is the cross-

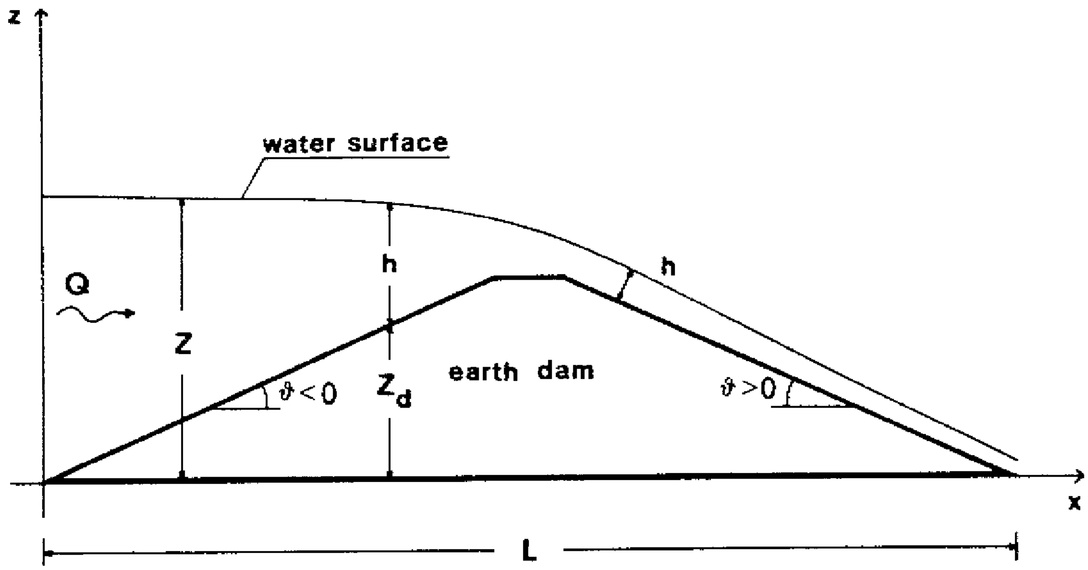


FIGURE 1 *Definition sketch*

sectional area of bed deposit, $Z$ is the water surface elevation, $S_f$ is the friction slope, $g$ is the acceleration due to gravity and $x$ and $t$ are, respectively, the longitudinal space co-ordinate and the time. The friction slope can be expressed with one of empirical equations for open channel resistance: $S_f = Q^2/K^2$, where $K$ is the conveyance factor.

Together with the continuity and dynamic equations for water flow a continuity equation is used for sediment:

$$\frac{\partial G_s}{\partial x} + \gamma_s(1-\lambda)\frac{\partial A_d}{\partial t} + \frac{\partial}{\partial t}(A\,C_s) = 0 \tag{3}$$

where $G_s$ is the solid discharge, $C_s$ is the suspended sediment concentration and $\gamma_s$ and $\lambda$ are, respectively, the specific weight and the porosity of sediment on the bed.

The set of partial differential Equations (1), (2), (3) links the three unknown functions $Q$, $Z$ and $A_d$ with independent variables $x$ and $t$ and can be solved with suitable boundary and initial conditions. At the upstream section it is possible to give three kinds of boundary conditions: the discharge $Q(t)$, the water surface elevation $Z(t)$ or a stage-discharge relationship.

In dynamic reservoir routing such an upstream condition is usually given by a continuity equation applied to reservoir storage volume $W$:

$$\frac{dW}{dt} = Q_i - Q_s - Q \tag{4}$$

where $Q_i$ is the inflow to the reservoir, $Q_s$ is the outflow due to spillways and $W$ is linked to $Z$ by a storage-elevation relationship.

Since the flow will be subcritical upstream and supercritical downstream a further condition is needed:

$$Fr^2 = \frac{Q^2B}{gA^3} = 1 \tag{5}$$

where $B$ is the width of cross-section at free surface elevation and $Fr$ is the Froude number. Equation (5) will be the second boundary condition for the upstream subcritical flow. The computed values of $Q$ and $Z$ at the last subcritical flow section will give the two boundary conditions for the downstream supercritical flow.

As regards erosion, the boundary condition in the first upstream section can be simply given by $A_d = 0$.

Water profile at $t = 0$ is evaluated as a steady, gradually varied flow, although this assumption is only a rough approximation of the actual initial condition.

## Sediment Transport Equation

The evaluation of the solid discharge $G_s$ can be obtained from one of the several sediment transport formulas developed for open channels (Vanoni, 1975).

However, it is important to point out that the conditions in which movement of sediment occurs during erosion of dams are very different from those for which the formulae have been calibrated.

In fact, during overtopping water flow is far from uniform, sediment transport is not in equilibrium conditions and shear stress can reach extremely high values.

Furthermore, for embankments built up with a clay core, during overtopping a mixture of cohesive and cohesionless material is eroded. In such conditions the sediment transport process needs further study.

## Numerical Approach

The simulataneous integration of the three partial differential Equations (1), (2), (3) is rather difficult.

However, in the case here analyzed it is possible to uncouple the Equation (3) from the system. Therefore, the solution of the system can be found solving, for each computational time step, first the De Saint Venant equations and then the sediment continuity equation (Chen *et al.*, 1975).

Concerning downstream supercritical flow, moreover, the unsteadiness of the water movement is due mainly to erosion so, during each time step, it can be considered as steady and computed, from critical section to downstream, as follows (Chow, 1959):

$$\frac{dh}{dx} = \frac{\tan\theta - S_f/\cos\theta}{\cos\theta - h\sin\theta\, d\theta/dh - Fr^2} \tag{6}$$

where $h$ is the water depth and $\theta = \theta(x)$ is the bottom slope (Figure 1).

During the erosion process the condition (5) has always been located in the section having the maximum bottom elevation. Such a condition has allowed to reproduce the actual behaviour of water flow.

Numerical integration of the Equations (1), (2) and (3) has been made using the finite difference method. The De Saint Venant equations and the sediment continuity equation have been discretized and linearized, respectively, according to the Preissmann implicit scheme and the linear centre implicit method.

Particular attention has been paid to the choice of space and time steps, as well as to the choice of the weighting coefficient of the Preissmann scheme, in order to avoid numerical instability in the reach where the Froude number is close to one. Moreover, in the downstream reach the best results have been achieved by introducing a smoothing technique for bottom profile.

## Model Verification

The effectiveness of the mathematical model suggested here has been checked on the basis of laboratory experiments carried out in the EDF National Hydraulic Laboratory, Chatou, France. The experience here considered concerns the erosion of a sand-dyke model described by Benoist and Nicollet (1983).

It has been found that the ability of the mathematical model to simulate the experimental data strongly depends on sediment transport formula adopted for $G_s$ estimation. The best results have been achieved by neglecting suspended transport and adopting the Meyer-Peter and Mueller (1948) formula:

$$\phi = 8(\tau^\star - \tau^\star_c)^{3/2} \tag{7}$$

where $\tau^\star$ and $\tau^\star_c$ are, respectively, the dimensionless shear stress and its critical value, and where:

$$\phi = \frac{G_s/B}{\gamma_s d\sqrt{\gamma' g d}} \tag{8}$$

with $d$ mean sediment diameter, $\gamma' = (\gamma_s - \gamma)/\gamma$ and $\gamma$ water specific weight. Since the slope of sand-dyke profile is not small, the critical dimensionless shear stress has been modified according to:

$$\tau^\star_c = \tau^\star_{co}\cos\theta(1 - \tan\theta/\tan\varphi) \tag{9}$$

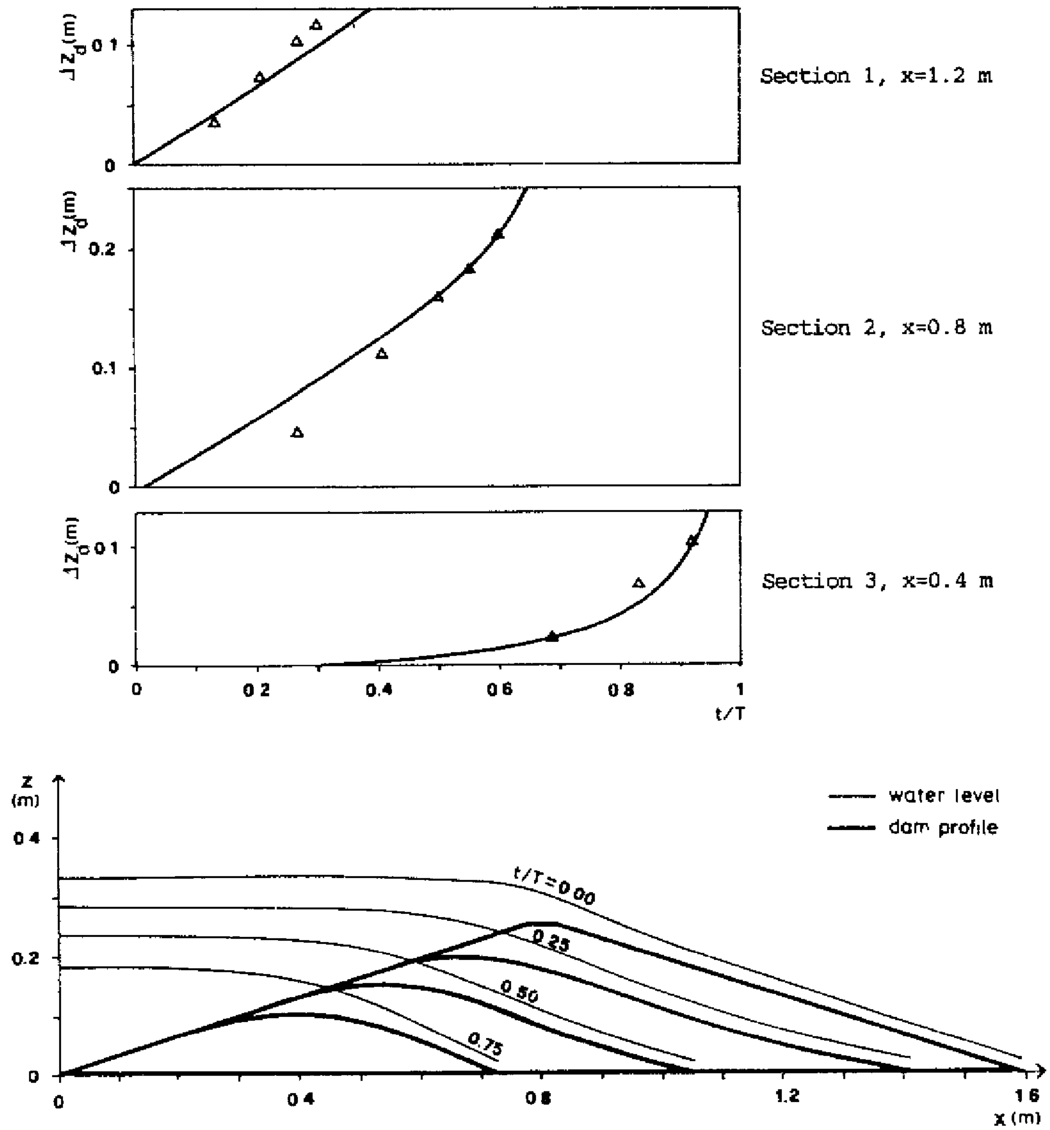


FIGURE 2 *(a) – Comparison between model results and experimental data, $T$ = complete erosion time, $\Delta Z_d$ = sand-dyke erosion. △, observed (Benoist and Nicollet, 1983), —, simulated (with Meyer-Peter and Mueller formula). Top: $x = 1.2$ m; middle: $x = 0.8$ m; bottom: $x = 0.4$ m. (b) – Simulated development of water levels (fine line) and dam profiles (heavy line)*

where $\varphi$ is the submerged angle of repose of the material and $\tau\star_{co}$ is the critical dimensionless shear stress on horizontal bed.

Figure 2(a) compares, on three dam sections, model outcome and experimental data. A good agreement between computed and observed erosion is obtained except for the middle dam section at the beginning of erosion. This is, perhaps, due to initial conditions employed in the mathematical model that might not reproduce the experimental conditions exactly.

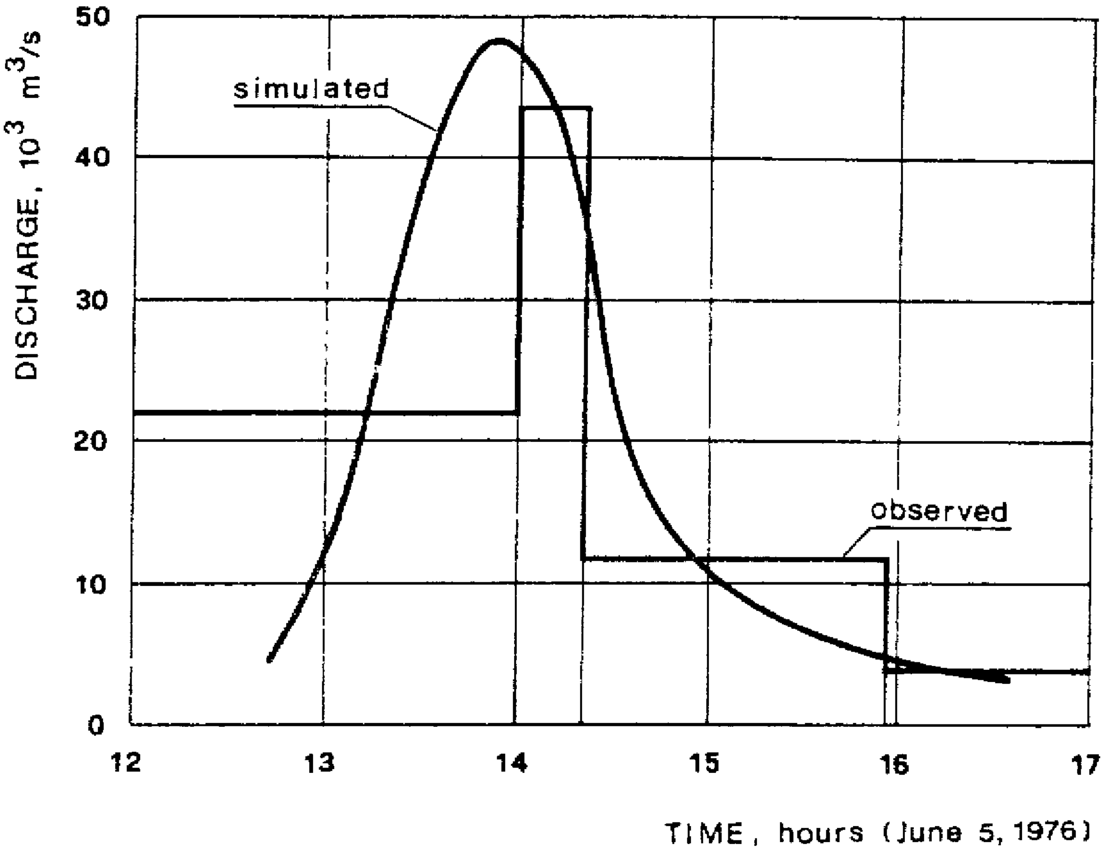


FIGURE 3 *Simulation of the outflow hydrograph due to Teton Dam Failure*

The simulated development of water and dam profiles are depicted in Figure 2(b).

## Model Application

The model has been applied to simulate the outflow hydrograph of the failure of Teton Dam, Idaho, USA. Field data, including observations of reservoir elevation during the failure, have been reported by Ray and Kjelstrom (1978).

Figure 3 shows the computed outflow hydrograph compared with the hystograph obtained with reservoir volume differentials and corresponding mean discharge. The agreement is very satisfactory and the simulated peak discharge according to the value estimated by Balloffet and Scheffler (1982).

Model results have been achieved by multiplying the solid discharge given by Meyer-Peter and Mueller formula by a factor of 2.4. The value of this factor, however, is strongly affected by the assumption, somewhat arbitrary, relative to breach geometry and then must be considered as a calibration parameter without a clear physical meaning.

## Conclusions

The phenomenon of earth dam failure due to overtopping is described, analyzing the unsteady flow of water over the embankment and the resulting erosion process.

The proposed mathematical model has been verified on the basis of laboratory experiments reported in the literature and it has given a good fitting of experimental data.

The application of the model to an actual dam failure has provided a satisfactory simulation of the observed outflow hydrograph.

Therefore, the model can be considered as a useful tool for earth dam breaching analysis and, even if depending on a careful calibration, can provide a realistic outflow hydrograph prediction.

## REFERENCES

BALLOFFET, A. and SCHEFFLER, M.L (1982) Numerical analysis of the Teton Dam failure flood. *J Hydraul Res* **20**: 317–328

BENOIST, G. and NICOLLET, G. (1983) Rupture progressive des barrages en terre. Proceedings XX IAHR Congress, Moscow, Vol II, 464–470

CHEN, Y.H., HOLLY, F.M., MAHMOOD, K. and SIMONS, D.B. (1975) Transport of material by unsteady flow. In: *Unsteady flow in open channels.* Yevjevich, V. and Mahmood, K. (Eds) Vol I. Water Resources Publications, Fort Collins, Colorado, pp. 313–365

CHOW, V.T. (1959) *Open channel hydraulics.* McGraw-Hill, New York, 680 pp

JOHNSON, F.A and ILLES, P. (1976) A classification of dam failures. *Water Power Dam Constr* **28**: 43–45

LEBRETON, A. (1985) Les ruptures et accidents graves de barrages de 1964 à 1983. *La Houille Blanche* **6/7**: 529–544

McDONALD, T.C. and LANGRIDGE-MONOPOLIS, J. (1984) Breaching characteristics of dam failures. *Proc ASCE J Hydraul Eng* **110**: 567–586

MEYER-PETER, E. and MUELLER, R. (1948) Formulas for bed-load transport. Proceedings II IAHR Meeting, Stockholm, pp. 39–64

RAY, H.A. and KJELSTROM, L.C. (1978) The flood in southeastern Idaho from the Teton Dam failure of June 5, 1976. U.S. Geological Survey, Open File Report 77–765.

SEED, H.B., MAKDISI, F.I. and DE ALBA, P. (1980) The performance of earth dams during earthquakes. *Water Power Dam Constr* **32**: 17–27

SHERARD, J.L., WOODWARD, R.T., GIZIENSKI, S.F. and CLEVENGER, W.A (1963) Earth and earth-rock dams. Wiley, New York, 725 pp

VANONI, V.A. (ED.) (1975) Sedimentation engineering. *ASCE Man Rep Eng Prac* **54**: 745

WURBS, R.A. (1987) Dam-breach flood wave models. *Proc ASCE, J Hydraul Eng* **113**: 29–46